CHAPTER 90

THE BOTTLENECK PROBLEM FOR TURBULENCE IN RELATION TO SUSPENDED SEDIMENT IN THE SURF ZONE

Peter Justesen[1], Jørgen Fredsøe[2] and Rolf Deigaard[3]

ABSTRACT

In the present paper the vertical distribution of turbulent kinetic energy k under broken waves is calculated by application of a one-equation turbulence model. The contributions to the energy level originate partly from the production in the wave boundary layer, partly from the production in the roller. Further on, the findings for k are used to calculate the vertical distribution of suspended sediment in broken waves.

INTRODUCTION

The vertical distribution of suspended sediment in the surf zone is of major importance for the evaluation of the rate of the longshore as well as the on-offshore sediment transport.

Outside the point of breaking, see Fig. 1, the presence of suspended sediment is restricted to the thin wave boundary layer. Models to describe this have been developed among others by Bakker (1974), Grant and Glenn (1983) and Fredsøe, Andersen and Silberg (1985).

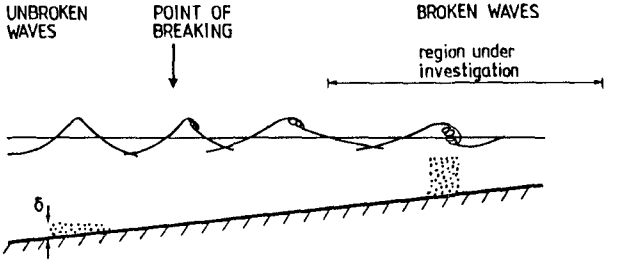

Fig. 1. Development of spilling breaker in the surf zone.

[1] M.Sc., Institute of Hydrodynamics and Hydraulic Engineering (ISVA), Technical University of Denmark, Building 115, DK-2800 Lyngby, Denmark.

[2] Ph.D., Dr. Techn., Professor in Marine Hydraulic Engineering, ISVA, Technical University of Denmark.

[3] Ph.D., Senior Hydraulic Engineer, Danish Hydraulic Institute, Agern Alle 5, DK-2970 Hørsholm, Denmark.

Inside the point of breaking, the surface generated turbulence results in a much higher level of turbulent kinetic energy, especially close to the water surface, where the production of turbulence takes place around the surface roller. This leads to a significant increase in the amount of suspended sediment compared to unbroken waves of same height and period on the same water depth.

In the present paper, we consider the conditions for fully developed broken waves, where the energy loss can be approximated by that in a hydraulic jump. (Turbulent bore).

The transition region from breaking to fully developed broken waves is not included in the present analysis. In case of a plunging breaker, the turbulence may be extremely violent at the location where the breaking wave splashes through the water surface. Until now, this flow has not been satisfactorily described. In case of a spilling breaker, the present theory may be modified to describe also the region between breaking and fully broken waves. This will however require a more detailed description of the development of the surface roller during the initial stages of breaking.

SCOPE OF PRESENT WORK

The main purpose of the present paper is to include a detailed description of the distribution of turbulence in the analysis of the suspended sediment, especially in the overlap region close to the bottom where contributions to the turbulence level originate from the surface roller as well as from the near-bed wave boundary layer.

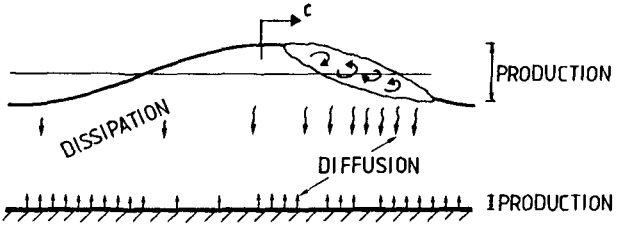

Fig. 2. Sketch of the location of production, diffusion, and dissipation of turbulent kinetic energy.

A first approach to solve this problem by application of a one-equation turbulence model for turbulent kinetic energy was proposed by Deigaard et al. (1986). In their model only the production of turbulence originating from wave breaking was included. Because this term is relatively well defined, the equation of motion could be avoided in the evaluation of the production term. As a result, the bottom generated turbulence was not directly included in the description, and Deigaard et

al. calculated the turbulence in the wave boundary layer independently using a simple model by Fredsøe (1984), in which the memory in turbulence is not included.

Because of the small thickness of the wave boundary layer, this might be a plausible approximation. However, the problem is how to combine the two contributions to get the total eddy viscosity. In Deigaard et al. (1986), the total eddy viscosity ε was estimated by

$$\varepsilon^2 = \varepsilon_b^2 + \varepsilon_t^2 \qquad (1)$$

where ε_b = eddy viscosity formed by production of energy in the wave boundary layer and ε_t = eddy viscosity formed by the production of energy in the water surface. Eq. 1 corresponds to summation of turbulent kinetic energy from the wall and the surface, respectively.

Especially in the overlap region where the level of turbulent kinetic energy is determined by both the surface and bed-generated turbulence a refined modelling of the level of k is needed. We refer to this region as the "bottleneck" region, because the level at this position is of extreme importance for how much sediment will be carried upwards to levels with higher turbulence. In the present theory, we use the transport equation for k to determine the distribution of k over the total depth. This analysis renders Eq. 1 redundant.

The advantage of the model by Fredsøe (1984) is that it is able to in a straightforward way to include the contribution of ε_b from a coexisting current in a three-dimensional motion. In this paper, the existence of such a current is disregarded. However, the present model can be extended to cover the combined wave current motion as long as this motion is restricted to a two-dimensional motion, see Deigaard, Justesen and Fredsøe (1986).

In the following description of the hydrodynamics and behaviour of suspended sediment, the bed is assumed to be plane and hydraulically rough. This restricts the present analysis to high values of the Shields parameter $\theta(> 1)$, according to Nielsen (1979). However, under storm conditions, where major parts of sediment transport takes place, this requirement is normally fulfilled.

HYDRODYNAMIC DESCRIPTION

Several attempts have been made in the past to describe the turbulence in the surf zone. Battjes (1975) has made a depth-integrated model for the turbulent kinetic energy and the eddy viscosity by assuming local equilibrium between the loss of energy from the waves and the dissipation of the turbulent energy. Svendsen and Madsen (1984) and Madsen and Svendsen (1983) applied the transport equation for turbulent kinetic energy to describe the longitudinal variation of the turbulence in a hydraulic jump or a bore. In this paper we shall calculate the eddy viscosity needed for the sediment calculations by use of the flow equation coupled with the transport equation for turbulent kinetic energy.

The flow kinematics are described by the equation of motion, which, neglecting convective terms, reads:

$$\frac{\partial U}{\partial t} = -\frac{1}{\rho}\frac{\partial p}{\partial x} + \frac{1}{\rho}\frac{\partial \tau}{\partial y} \tag{2}$$

U is the horizontal velocity, p is the pressure, and τ is the shear stress. The eddy viscosity ε is defined by

$$\frac{\tau}{\rho} = \varepsilon \frac{\partial U}{\partial y} \tag{3}$$

The turbulence is described by a one-equation turbulence model using the transport equation for the turbulent kinetic energy, k:

$$\frac{\partial k}{\partial t} = \frac{\partial}{\partial y}\left(\frac{\varepsilon}{\sigma_k}\frac{\partial k}{\partial y}\right) + \frac{PROD}{\rho} - C_1 \frac{k^{3/2}}{\ell} \tag{4}$$

According to Launder and Spalding (1972), the Prandtl number σ_k and the dissipation coefficient C_1 are taken to be $\sigma_k = 1$ and $C_1 = 0.08$. The length scale of the turbulence is to be prescribed. In the present model we have used ℓ given by:

$$\ell = \begin{cases} \sqrt[4]{C_1}\kappa y & \text{for } y < 0.07\,\dfrac{D}{\sqrt[4]{C_1}\kappa} \\ 0.07D & \text{for } y > 0.07\,\dfrac{D}{\sqrt[4]{C_1}\kappa} \end{cases} \tag{5}$$

κ is von Karman's constant ($\kappa = 0.40$). Close to the bed, ℓ has the variation normally used for boundary layer modelling, whereas it attains a constant value away from the bed to describe the conditions of free turbulence.

The coefficient of momentum diffusion, the eddy viscosity ε, is determined by the turbulent energy and the length scale:

$$\varepsilon = \ell \sqrt{k} \tag{6}$$

The production term, PROD, in the transport equation has two contributions. The first one is the production derived from the flow equation:

$$PROD = \tau \frac{\partial U}{\partial y} \tag{7}$$

This part of the turbulent production is most important in the wave boundary layer.

The second contribution is from the wave breaking. The details of the flow pattern in the surface roller is not modelled by the hydrodynamic model, and the production of turbulence in the surface roller is included in the transport equation by an analytical approximation introduced by Deigaard et al. (1986). The total energy dissipation due to the wave breaking is estimated from the energy loss in a hydraulic jump with the same height as the waves. The location of the production of turbulence is prescribed in the model on the basis of turbulence measurements in hydraulic jumps presented by Rouse et al. (1958). The turbulence originating from the wave breaking is dominant in the main part of the flow outside the wave boundary layer.

The boundary conditions for the k-equation are the no-flux condition at the surface:

$$\frac{\partial k}{\partial y}\Big|_{y=D} = 0 \tag{8}$$

and

$$k(z_0,t) = \frac{1}{\sqrt{C_1}}\,\varepsilon\,\left|\frac{\partial U}{\partial y}\right|,\quad z_0 = \frac{k_N}{30} \tag{9}$$

which expresses local equilibrium near the bed between production and dissipation of turbulent energy. k_N = bed roughness in Eq. 9. In addition, periodicity in the solution is required.

The pressure gradient in the flow equation is given by the free stream velocity, U_0:

$$\frac{1}{\rho}\frac{\partial p}{\partial x} = -\frac{\partial U_0}{\partial t} \tag{10}$$

The free stream velocity is estimated from linear shallow water theory:

$$U_0 = U_{1m}\sin\left(\frac{2\pi}{T}t\right) \tag{11}$$

By introducing these relations the following equation of motion is obtained:

$$\frac{\partial(U-U_0)}{\partial t} = \frac{\partial}{\partial y}\left(\varepsilon\frac{\partial U}{\partial y}\right) \tag{12}$$

The boundary conditions are (i) the no-slip condition at the bed

$$U(z_0,t) = 0 \tag{13}$$

and (ii) vanishing shear stress at the surface

$$\frac{\partial U}{\partial y}\Big|_{y=D} = 0 \tag{14}$$

Furthermore, periodicity in time is required.

THEORETICAL FLOW RESULTS

Two examples of the calculated instantaneous picture of the turbulent kinetic energy level for $a/k_N = 10^2$ and $a/k_N = 10^4$ are shown on the left hand side of Figs. 3 and 4, respectively. The production of surface generated turbulence has been set to zero in Figs. 3A and 4A in order to study the bed generated turbulence in the wave boundary layer alone. a = is the free stream amplitude and k_N the bed roughness. The variation in the x-direction (the direction of wave propagation) is obtained from the time variation by use of the relation

$$\frac{\partial}{\partial x} = -\frac{1}{c}\frac{\partial}{\partial t} \tag{15}$$

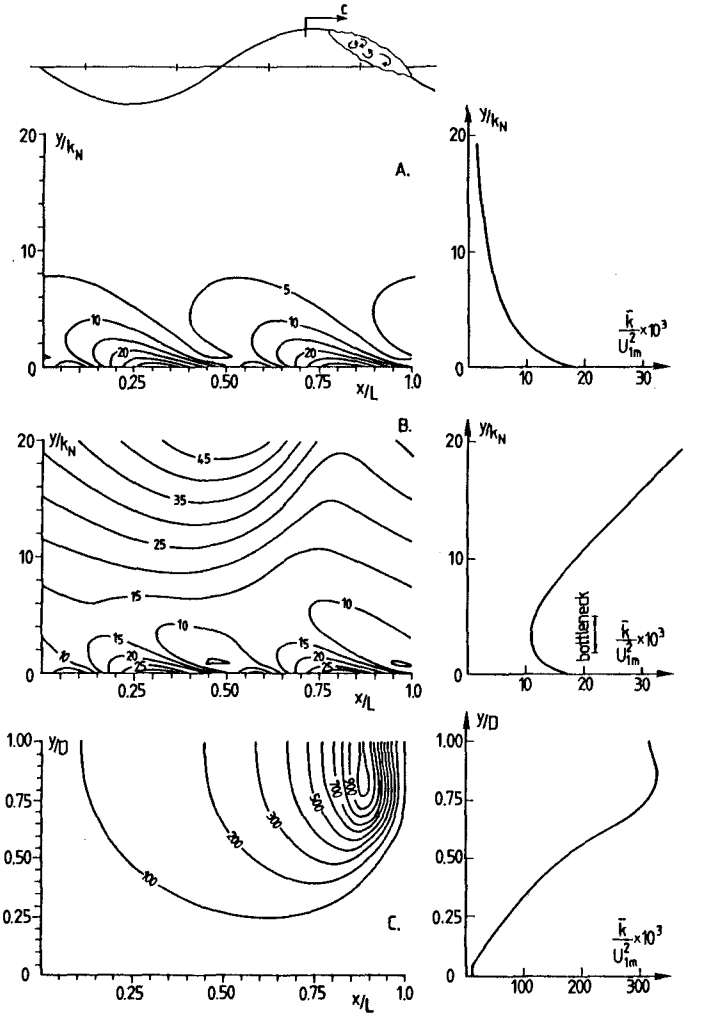

Fig. 3. Calculated distribution of turbulent kinetic energy (TKE) in unbroken and broken waves. Contour plots show the temporal variation of TKE, and the corresponding time-averaged levels of TKE are depicted on the right. A: Unbroken wave only with bottom-generated TKE; B: Near-bed region in broken wave; C: Total depth in broken wave. $a/k_N = 10^2$, $gT^2/D = 300$, $H/D_k = 0.5$. Levels of TKE indicated on contours are $\frac{\bar{k}}{U_{1m}^2} \times 10^3$.

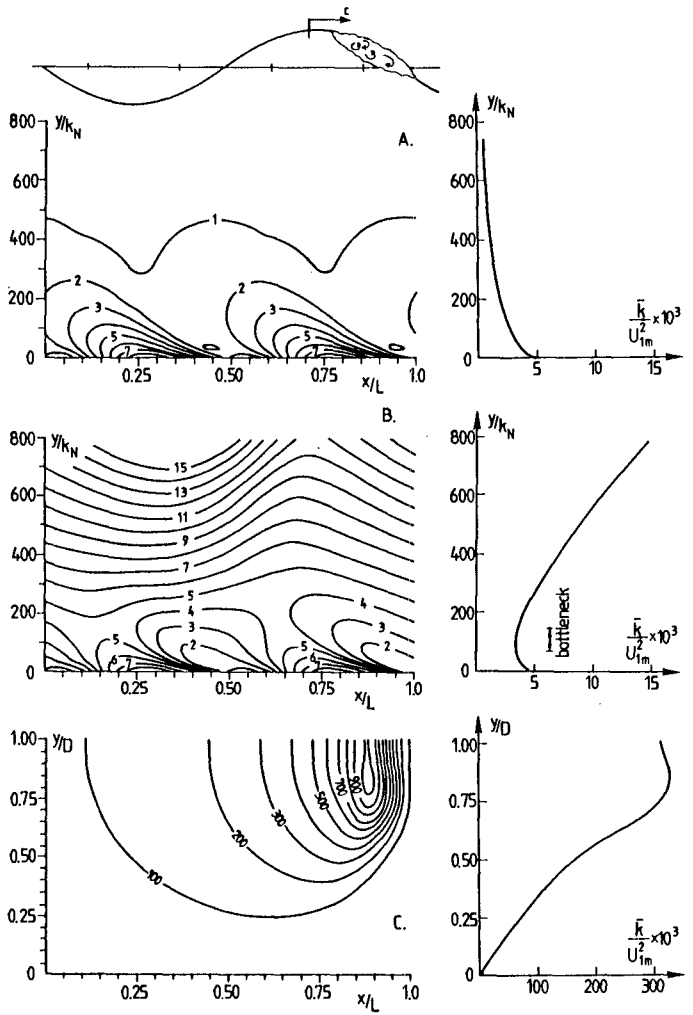

Fig. 4. Same as Fig. 3, but for $a/k_N = 10^4$, $gT^2/D = 300$, $H/D = 0.5$

It is seen that k has a maximum at the bottom, where the main production takes place. The shape of the contour plot is skew because it takes some time for the eddies to decay after being formed (mainly at the large outer flow velocities). The skewness is especially pronounced for small values of a/k_N, where the flow reverses rapidly. The pictures shown in Figs. 3A and 4A are experimentally verified by Hino et al. (1983) in case of a hydraulically smooth bottom.

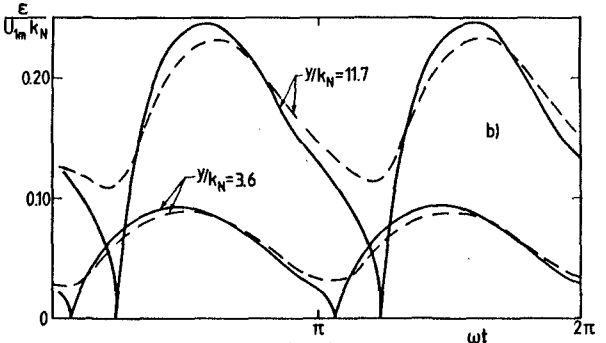

Fig. 5. Calculated temporal variation of eddy viscosity during one wave cycle in unbroken wave. - - - : one-equation model; —— : mixing-length theory. $a/k_N = 10^3$.

Fig. 5 shows the variation in the eddy viscosity during a wave cycle. The eddy viscosity is found from Eq. 6, and the importance of including a description of the behaviour of k is illustrated in Fig. 5 by comparing the predictions of a one-equation model with those of a mixing-length model, Bakker and van Doorn (1978). The implications of including a one equation model in the description of k are twofold: A: the time variation in ε is now predicted to be much smaller, because it takes time for the turbulent kinetic energy to decay, and B: the turbulence intensity increases further away from the bed at small values of a/k_N, because the turbulence level can now be built up with time.

In Figs. 3B, 3C and 4B and 4C contour plots of the instantaneous level of k, including the effect of turbulence formed around the roller, are shown. While the bottom turbulence has two peaks during one wave cycle (due to maximum flow velocity back and forth, respectively) the top generated surface has only one peak, just below the roller. In Fig. B, the detailed contour plots close to the bottom are depicted, while Fig. C shows the conditions over the entire depth. It is seen that the turbulence level is much higher far away from the bed than close to the bed.

On the right hand side of Figs. 3 and 4, the corresponding time-averaged values of k are shown. It is quite clear that a minimum (bottleneck) in k is present very close to the bottom, inside the wave boundary layer. This minimum in k is especially pronounced just below the roller, because it takes some time for the turbulence to penetrate downwards from the roller.

DESCRIPTION OF SUSPENDED SEDIMENT

The description of the vertical distribution of suspended sediment is based on the diffusion concept, for which the governing equation is the well-known

$$\frac{\partial c}{\partial t} = w \frac{\partial c}{\partial y} + \frac{\partial}{\partial y}\left(\varepsilon_s \frac{\partial c}{\partial y}\right) \tag{16}$$

where c = concentration by volume, t = time, w = fall velocity of suspended sediment, and ε_s = turbulent exchange factor for suspended sediment. In Eq. 16 the lateral diffusion term is neglected because the vertical gradient is much larger than the horizontal. ε_s is usually correlated to the eddy viscosity ε by

$$\varepsilon_s = \beta\varepsilon \tag{17}$$

where β is a constant of proportionality. Quite often, β is set equal to unity. Some experimental findings by van der Graaff and Roelvink (1984) suggest, however, that β is a function of the sediment properties: β increases with increasing grain size, and is normally somewhat larger than unity.

In the following calculations we have applied $\beta = 1$, so

$$\varepsilon_s = \varepsilon \tag{18}$$

If another value of β in Eq. 18 is adopted, the present results can still be applied by introducing a new fictive fall velocity

$$w_n = w\beta \tag{19}$$

because the vertical distribution depends only on the relative ratio w/ε_s.

Boundary condition at the bed: One of the major problems in steady current as well as in wave motion is to determine the bottom concentration c_b of suspended sediment. Here c_b is defined as the concentration of sediment a distance of about one to two grain diameters above the bed. Einstein (1950) suggested a kinematic approach, where the concentration of suspended sediment just above the bottom is directly related to the rate of the bed load transport.

Engelund and Fredsøe (1976) developed a model for c_b based on dynamic principles, describing how the fluid shear stress is transferred to the immobile part of the bed through the dispersive stress of the grains in suspension. An experimental result for the dispersive stress obtained by Bagnold (1954) was applied to calculate c_b.

The variation in c_b is obtained as a function of the Shields parameter, defined by

$$\theta = \frac{U_f^2}{(s-1)gd} = \frac{\tau_b}{\rho(s-1)gd} \tag{20}$$

s = relative density (2.65 for sand), g = acceleration due to gravity, d = mean grain diameter), cf. [8].

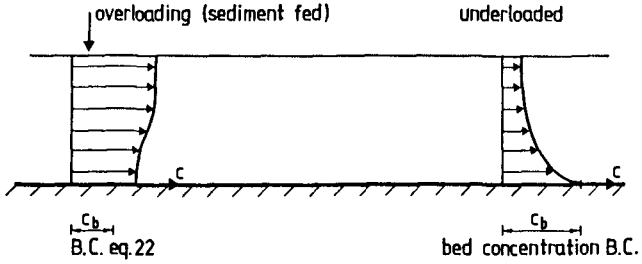

Fig. 6. Definition sketch of boundary condition for sediment concentration.

In two recent papers on suspended sediment in waves by Fredsøe et al. (1985) and Deigaard et al. (1986) the above mentioned method was applied to calculate the instantaneous value of c_b, based on the instantaneous value of θ

$$c_b = c_b(\theta) \tag{21}$$

The application of Eq. 21 seems reasonable from a physical point of view, since the theory behind the estimate of c_b is based on the assumption that c_b must have a certain value in order to transfer the fluid shear to the bed. However, in connection with a related topic, namely non-uniform river flow, Parker [16] discussed the above boundary condition, which he denotes the concentration boundary condition. In case of non-zero flux conditions, (i.e. erosion or deposition occurs in the bed) Parker instead applied a gradient boundary condition. This boundary condition was introduced because Eq. 21 gives physically unrealistic results in the case of overloading.

Let us consider the hypothetic case, in which the flow velocity is suddenly reduced from a certain steady value where $\theta = \theta_0$ to zero: in this case, Eq. 21 gives the result that c_b drops from $c_b(\theta_0)$ to zero instantaneously. However, all the sediment which is in suspension before the change in flow velocity occurs cannot settle faster than the settling velocity w. This means that in the still water, the time evolution in c_b is determined by

$$c_b(a,t) = c(a + \Delta y, t - \Delta t) \tag{22}$$

in which $\Delta y = w\Delta t$.

This equation simply states that the suspended sediment settles without changing its shape of the profile.

The example described above corresponds to the overloaded case. The underloaded case corresponds on the other hand to the flow situation where the fluid velocity is suddenly increased from zero to a certain flow velocity where $\theta = \theta_0$: here, it is possible for the bed concentration to adapt the new value $c_b(\theta_0)$ (disregarding inertia effects, which for sand are negligible)

because the suspended sediment just has to be transported a very small distance of the order of one grain diameter away from the bed. In this case, the sediment is not transported by diffusion, but by grain-grain interaction.

If we apply these considerations to the unsteady case under waves, an alternative boundary condition to the boundary condition Eq. 21 is

Underloading: Eq. 21

Overloading: Eq. 22

so the resulting boundary conditions become

$$c_b = \max \{c_b(\theta),\ c(a + w\Delta t,\ t - wt\} \tag{23}$$

In the wave case where the changes in flow velocity are continuous, Eq. 23 is still applied, as it describes the two extreme limits (for very fast varying flow) correctly.

Boundary condition at the surface: at the free surface, the flux of sediment is zero, or

$$\epsilon \frac{\partial c}{\partial y} + wc = 0 \quad \text{at } y = D \tag{24}$$

Periodicity in concentration: the time variation in c must be periodic, so

$$c(t,y) = c(t + T,\ y) \tag{25}$$

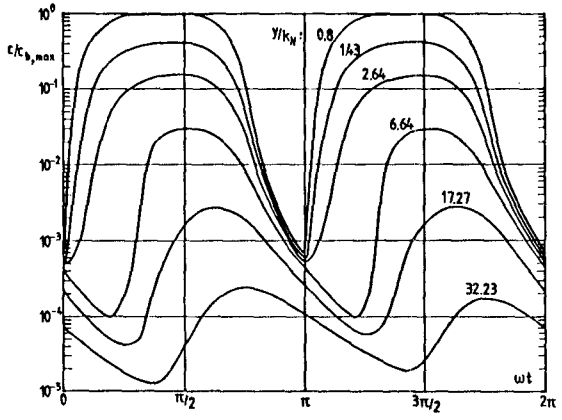

Fig. 7. Sediment concentration in different levels in a broken wave calculated as a function of time. $a/k_N = 10^3$, $gT^2/D = 300$, $H/D = 0.5$, $d = 0.2$ mm, $w/U_{1m} = 0.038$.

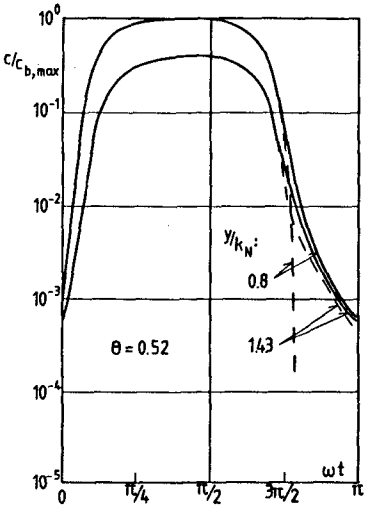

Fig. 8. Effect of choice of boundary condition for the sediment concentration. Solid lines indicate the same results as in Fig. 7 obtained using Eq. 23, whereas the dashed lines show results by using the bed concentration B.C.

THEORETICAL RESULTS FOR SUSPENDED SEDIMENT

Figs. 7 and 8 show the time-variation in the instantaneous value of concentration c of suspended sediment. It is noted from Fig. 7 that the concentration at a specific level is not totally identical in each wave half period. This can be explained by the former hydrodynamic calculations.

Fig. 8 shows the effect of the boundary condition selected: the dashed line in Fig. 8 is the result obtained by applying the bed concentration boundary condition, while the full drawn line is that obtained from Eq. 23. It is seen that the effect from different boundary conditions can be felt only a few grain sizes away from the bed.

Figs. 9 - 11 are related to the predicted vertical mean distribution c: in Fig. 9 the variation in c with a/k_N is depicted. The dashed line shows the results without wave breaking. In Figs. 10 and 11, the variation with gT^2/D and w/U_{1m}, respectively, are depicted.

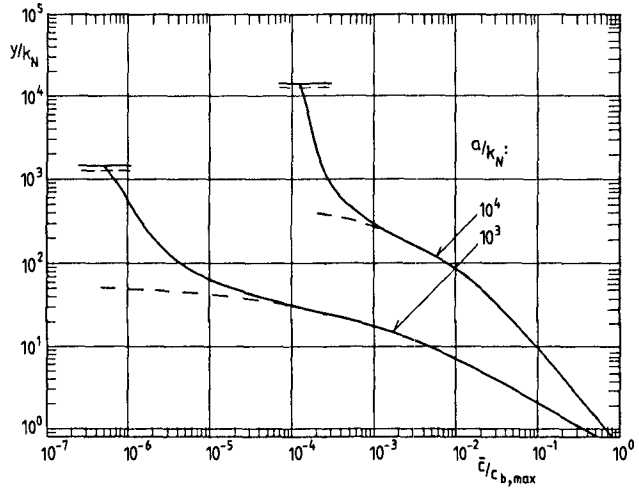

Fig. 9. Time-averaged concentration of suspended sediment as a function of depth for different values of a/k_N. GT^2/D = 300, H/D = 0.5, d = 0.2 mm, w = 0.025 m/s. Dashed lines indicate results for unbroken waves.

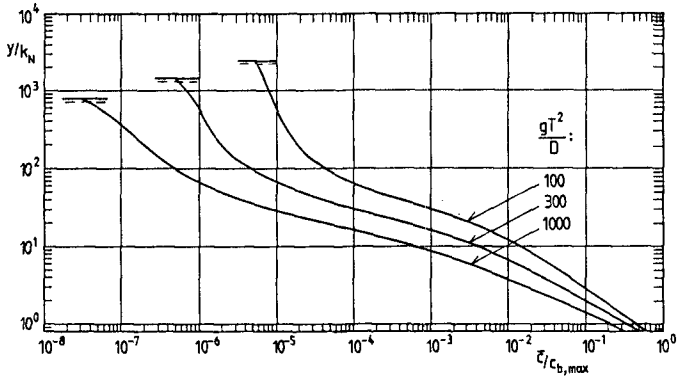

Fig. 10. Time-averaged concentration of suspended sediment as a function of depth for different values of gT^2/D. a/k_N = 10^3, H/D = 0.5, d = 0.2 mm, w = 0.025 m/s.

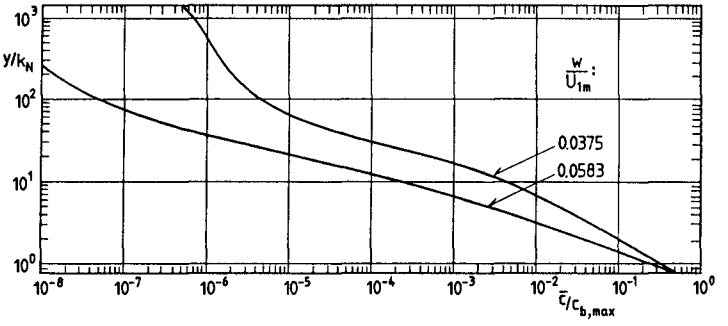

Fig. 11. Time-averaged concentration of suspended sediment as a function of depth for different values of w/U_{1m}. $a/k_N = 10^3$, $gT^2/D = 300$.

REFERENCES

[1] Bagnold, R.A.: "Experiments on a gravity-free dispersion of large solid spheres in a Newtonian fluid under shear". Proceedings, Royal Society, London, England, Ser. A., 225, p. 49, 1954.

[2] Bakker, W.T.:" Sand concentration in an oscillatory flow". Coastal Engineering Conference, pp. 1129-1148, 1974.

[3] Bakker, W.T. and van Doorn, Th.: "Near-bottom velocities in waves with a current". Coastal Engineering Conference, pp. 1394-1413, 1978.

[4] Battjes, J.A.: "Modeling of turbulence in the surfzone". Proc. Symposium on modeling Techniques. ASCE, San Francisco, California, 1975.

[5] Deigaard, R., Fredsøe, J. and Hedegaard, I.B.: "Suspended sediment in the surf zone". J. Waterway, Port, Coastal and Ocean Engineering. Vol. 112, No. 1, pp. 115-128, 1986.

[6] Deigaard, R., Justesen, P. and Fredsøe, J.: "Two-dimensional circulation in the surf zone". Submitted for possible publication. 1986.

[7] Einstein, H.A.: "The bed load function for sediment transportation in open channels". U.S. Dept. Agriculture, Technical Report, p. 1026, 1950.

[8] Engelund, F. and Fredsøe, J.: "A sediment transport model for straight alluvial channels". Nordic Hydrology, Vol. 7, pp. 293-306, 1976.

[9] Fredsøe, J.: "Turbulent boundary layer in wave and current motion". J. Hydraulic Engineering, ASCE, Vol. 110, No. 8, pp. 1103-1120, 1984.

[10] Fredsøe, J., Andersen, O.H. and Silberg, S.: "Distribution of suspended sediment in large waves". J. Waterway, Port, Coastal and Ocean Engineering, ASCE, Vol. 111, No. 6, pp. 1041-1059, 1985.

[11] Grant, W.G. and Glenn, S.M.: "Continental shelf bottom boundary layer model, Vol. I: Theoretical model development". Woods Hole Oceanographic Institution, Ocean Engineering Dept., 1983.

[12] Hino, M., Kashiwayanagi, M.O.B.S., Nakayama, A. and Hara, T.: "Experiments on the turbulence statistics and the structure of a reciprocating oscillatory flow". J. Fluid Mech., Vol 131, pp. 363-400, 1983.

[13] Launder, B.E. and Spalding, D.B.: "Mathematical models of turbulence". Academic Press, London and New York, 1972.

[14] Madsen, P.Å and Svendsen, I.A.: "Turbulent bores and hydraulic jumps". J. Fluid Mech., Vol. 129, pp. 1-25, 1983.

[15] Nielsen, P.: "Some basic concepts of wave sediment transport". Institute of Hydrodynamic and Hydraulic Engineering, Technical University of Denmark, Series Paper 20, 1979.

[16] Parker, G.: "Self-formed straight rivers with equilibrium banks and mobile bed. Part 1: The sand river." J. Fluid Mech., Vol. 89, 1, pp. 109-126, 1978.

[17] Rouse, H., Siao, T.T. and Nagaratnam, S.: "Turbulence characteristics of the hydraulic jump". Proceedings, ASCE, Vol. 84, No. HY1, pp. 1-30, 1958.

[18] Svendsen, I.A. and Madsen, P.: "A turbulent bore on a beach". J. Fluid Mech., Vol. 148, pp. 73-96, 1984.

[19] Van de Graaff, J. and Roelvink, J.A.: "Grading effects in concentration measurements". Coastal Engineering Conference, pp. 1618-1631, 1984.